

# Density-functional approach to electron dynamics: Stable simulation under a self-consistent field

Osamu Sugino and Yoshiyuki Miyamoto

*Fundamental Research Laboratories, NEC Corporation, 34 Miyukigaoka, Tsukuba, Ibaraki-Ken, 305-8501, Japan*

(Received 30 July 1998)

We propose efficient and stable numerical methods for simulating the electron dynamics within the time-dependent density-functional theory and the nonlocal pseudopotential. In this scheme, time evolution of the wave function is followed by self-consistently solving the time-dependent Kohn-Sham equation using the higher-order Suzuki-Trotter type split-operator method. To eliminate the numerical instability problem and increase the time step for the integration, we introduce the railway curve scheme to interpolate the self-consistent potential and the cutoff schemes to smooth the kinetic energy operator and the charge density. Applying these techniques to the electron dynamics of an Al cluster and the electron-ion dynamics of an excited K cluster, we found that they significantly improve the stability and efficiency. This opens the possibility of performing subpicosecond-long simulations of the transient dynamics of electrons and ions for a number of materials. [S0163-1829(99)14403-5]

## I. INTRODUCTION

The transient dynamics of electrons and ions have become the target of extensive research owing to the development of experimental techniques such as the use of pulsed lasers.<sup>1</sup> Such research has led us to the discovery of details concerning, for example, ultrafast chemical reactions triggered by electron excitation,<sup>1</sup> or the transport and decay of carriers in bulk or nanostructures.<sup>2</sup> Theoretically, these reactions and the transport and decay of carriers can be studied by explicitly integrating the time-dependent many-body Schrödinger equation with respect to time, but this method of calculation is much less developed than time-independent methods. Recently, time-dependent density-functional theory (TD-DFT)<sup>3</sup> has attracted much attention because it offers a reasonable level of simplicity and accuracy. There have been several applications of this theory concerning the tunneling of electrons in mesoscopic quantum structures,<sup>4</sup> electron transfer in the collision of microclusters,<sup>5</sup> and the excitation spectra of molecules.<sup>6</sup> Most TD-DFT calculations simply adopt the adiabatic density functional for the exchange-correlation energy, though it does not include the memory effect.<sup>7-9</sup> When calculated results have been compared with those of an exact calculation on a two-electron system or with experimental results, however, a satisfactory description was found to have been given for several problems. Tunneling coefficients<sup>4</sup> and excitation energy<sup>6</sup> are two such examples.

Applying the TD-DFT to mixed electron-ion dynamics may not always be justified because of the well-known branching problem,<sup>10,11</sup> but such simulation can yield important information for carefully selected problems. The branching problem is known to be significant when electrons deviate from the adiabatic surface and the Hellmann-Feynman forces derived from each constituting adiabatic surface become different from each other.<sup>10,11</sup> Yet, there are ways to avoid this problem. First, by adopting the surface hopping prescription,<sup>12</sup> we can continue a simulation after the branching by letting the electrons return to one of the adiabatic surfaces. Such simulations have been done recently by several authors.<sup>13-15</sup> Second, the effect of the branching is usu-

ally less serious when studying the collision of energetic particles. Third, we can extract information regarding how fast and to which surface the electron jumps from the part of the simulation done before the branching problem becomes significant.

Several numerical difficulties, however, appear when extensively applying the TD-DFT. First, the time step for the integration,  $\Delta t$ , is several hundred times smaller than the one used by the Car-Parrinello type molecular dynamics (MD).<sup>16</sup> For example, for carbon,  $\Delta t$  was taken as  $6.6 \times 10^{-4}$  fs or 0.027 a.u.,<sup>6</sup> while  $\Delta t$  for the Car-Parrinello type MD is about 7 a.u. (Ref. 17). The number of operations thus differs by roughly three orders of magnitude. With such a small  $\Delta t$ , it is impractical to simulate for subpicosecond intervals, which is a typical time scale required to induce a chemical reaction. Second, the total energy, which is a constant of motion in our case, tends to significantly drift unless a prohibitively smaller  $\Delta t$  is used (see Sec. II below for examples). The drift often grows exponentially, and serious numerical instability eventually occurs. This problem does not appear in one-body calculations, but appears when the self-consistent potential is used. Therefore this is a problem inherent to many-body calculations such as in DFT and probably Hartree-Fock calculations.

In this context, our aim is to show how  $\Delta t$  can be increased while eliminating the numerical instability. We apply several numerical techniques: use of a higher-order Suzuki-Trotter type split operator<sup>18</sup> as is frequently used for quantum Monte Carlo simulation, cutoff of the kinetic and potential energy operators as is done for the Car-Parrinello<sup>16</sup> type plane-wave calculations, and the application of the railway (RW) curve interpolation<sup>19</sup> to update the self-consistent potential. In particular, the newly introduced RW scheme plays an important role in stabilizing the simulation. When these techniques are combined,  $\Delta t$  can be significantly increased without leading to numerical inaccuracy or instability. For example,  $\Delta t$  for Al and K becomes 0.5–1.0 a.u. and the number of operations becomes only about two orders of magnitude larger than that of the Car-Parrinello type MD. Below, we provide detailed formulations in Sec. I within the

TABLE I. Parameter set for the sixth- and eighth-order Suzuki-Trotter decomposition. The parameters determined by Suzuki (a) satisfy  $|p_i| < 1$  while those determined by Yoshida (b) do not.

		(a)			
6th $q=14$ ( $p_i=p_{15-i}$ )		8th $q=15$ ( $p_i=p_{16+i}$ )			
$p_1=p_2$	0.392256805387732	$p_1$	0.210902950774054	$p_5$	0.769771783843536
$p_3=p_4$	0.01177866066796810	$p_2$	0.835657990415923	$p_6$	0.199415314882502
$p_5=p_6$	-0.5888399920894384	$p_3$	-0.658440728286576	$p_7$	0.0363152045812476
$p_6=p_8$	0.06575931603419684	$p_4$	-0.0774373402366569	$p_8$	-0.0892171910150694
		(b)			
		6th $q=7$ ( $p_j=p_{8-j}$ )			
		$p_1$	0.784513610477560		
		$p_2$	0.0235573213359357		
		$p_3$	-1.17767998418887		
		$p_4$	1.31518632068391		

nonlocal pseudopotential scheme. In Sec. II we demonstrate the capabilities of these combined techniques by doing a subpicosecond simulation of simple molecules,  $\text{Al}_2$  and  $\text{K}_3$ .

## II. METHOD OF CALCULATION

### A. Suzuki-Trotter type split-operator method

In integrating the time-dependent Schrödinger (Kohn-Sham) equation, we use the Suzuki-Trotter type split-operator method.<sup>18</sup> The split-operator method was originally introduced by Feit and co-workers<sup>20</sup> to approximate the exponential of the Hamiltonian as a product of the exponential of the kinetic energy operator  $T$  and the potential energy operator  $V$  as

$$\exp[-i(T+V)\Delta t] \approx \exp\left[-\frac{1}{2}iT\Delta t\right] \exp[-iV\Delta t] \times \exp\left[-\frac{1}{2}iT\Delta t\right]. \quad (1)$$

The advantages of this method are as follows. First, since  $T$  and  $V$ , respectively, are diagonal in reciprocal space and real space, the exponential can be directly calculated. Second, since it keeps the unitarity of the time evolution, the orthonormality of the wave functions is guaranteed, allowing us to skip the time consuming orthonormalization operation. This is particularly advantageous when using parallel computers. Third, this scheme is unconditionally stable,<sup>21,22</sup> in that the simulation does not show divergent behavior even when  $\Delta t$  is too large. This is unlike other methods where the exponential is expanded into a series of  $H\Delta t$ .

Suzuki<sup>18</sup> generalized this method and provided higher-order schemes for decomposing operators that consisted of  $q$  components,  $H = \sum_{n=1}^q A_n$ . According to Suzuki's method, the exponential of  $H$  up to the second order of  $-i\Delta t$  ( $\equiv x$ ) can be approximated as

$$e^{xH} \approx e^{(x/2)A_1} e^{(x/2)A_2} \dots e^{(x/2)A_{q-1}} e^{xA_q} e^{(x/2)A_{q-1}} \dots e^{(x/2)A_2} e^{(x/2)A_1} \equiv S_2(x). \quad (2)$$

Using the second-order symmetric decomposition  $S_2(x)$ , higher-order decompositions can be constructed: For example, the fourth-order symmetric decomposition can be written as

$$S_4(x) = S_2(p_1x)S_2(p_2x)S_2(p_3x)S_2(p_2x)S_2(p_1x), \quad (3)$$

where the parameters  $p$  follow the equations

$$\begin{aligned} 2p_1 + 2p_2 + p_3 &= 1, \\ 2p_1^3 + 2p_2^3 + p_3^3 &= 0. \end{aligned} \quad (4)$$

The set of solutions

$$\begin{aligned} p_1 = p_2 &= \frac{1}{4 - 4^{1/3}}, \\ p_3 &= 1 - 4p_1 \end{aligned} \quad (5)$$

is a special one that minimizes  $\max[|p_1|, |p_2|, |p_3|]$ . The parameters obtained for the sixth- and eighth-order schemes are shown in Table I(a). The parameters  $p_j$  given by Suzuki satisfy  $|p_j| < 1$  for all  $j$ , while the parameters previously given by Yoshida<sup>23</sup> do not [see Table I(b)]. Minimizing the maximum  $|p_j|$  is known to be very important for Monte Carlo simulations where imaginary time is used, but we have found this is also advantageous when using real time.

Suzuki<sup>24</sup> also extended this scheme to the case containing time-dependent operators. (See also Ref. 25.) For example, the fourth-order decomposition can be written as

$$\begin{aligned} \hat{T} \left[ \exp \left( -i \int_t^{t+\Delta t} H(s) ds \right) \right] &= S_2(p_1x; t_1) S_2(p_2x; t_2) \\ &\quad \times S_2(p_3x; t_3) S_2(p_2x; t_4) \\ &\quad \times S_2(p_1x; t_5) + O(x^5), \\ S_2(x; t) &\equiv e^{(x/2)A_1(t)} e^{(x/2)A_2(t)} \dots e^{(x/2)A_{q-1}(t)} \\ &\quad \times e^{xA_q(t)} e^{(x/2)A_{q-1}(t)} \dots e^{(x/2)A_2(t)} e^{(x/2)A_1(t)}, \quad (6) \\ t_j &= t + (p_1 + p_2 + \dots + p_{j-1} + p_j/2)\Delta t, \end{aligned}$$

$$p_5 = p_1; p_4 = p_2,$$

where  $\hat{T}$  is the time-ordering operator.

When applying the split-operator method to the TD-DFT, the Suzuki-Trotter decomposition is suitable for several reasons. First, decomposition can be performed even for the nonlocal pseudopotential calculation where the Hamiltonian consists of many noncommutable potentials, the Hartree-exchange-correlation potential  $V_{\text{Hxc}}$ , and the nonlocal pseudopotentials  $V_{\text{nl}}$ . Second, since the  $V_{\text{Hxc}}$  is expected to be strongly dependent on time, the variation of the Hamiltonian between  $t$  and  $t + \Delta t$  should be explicitly taken into account unless a sufficiently small  $\Delta t$  is used. Third, to prevent a loss of phase information concerning the dynamics after a long simulation, numerical accuracy achieved by using a higher-order scheme is important.

### B. TD-DFT pseudopotential theory

We will briefly discuss the algorithm for the TD-DFT pseudopotential simulation. The electronic part of the Hamil-

tonian consists of the kinetic energy operator, the Hartree-exchange-correlation potential, and the pseudopotentials centered on each atom  $R_\tau$ ,

$$H = T + V_{\text{Hxc}}[\rho] + \sum_{\tau lm} V_{\tau lm}^{\text{ps}}(\mathbf{r} - \mathbf{R}_\tau), \quad (7)$$

where  $l$  and  $m$  stand for the angular and azimuthal quantum numbers, respectively. In the Kleinmann-Bylander form,<sup>26</sup> the nonlocal pseudopotential can be written as

$$V_{\tau lm}^{\text{ps}}(\mathbf{r}) = \frac{V_{\tau l}^{\text{ps}} |P_{\tau l} Y_{lm}\rangle \langle P_{\tau l} Y_{lm} | V_{\tau l}^{\text{ps}}}{\langle P_{\tau l} Y_{lm} | V_{\tau l}^{\text{ps}} | P_{\tau l} Y_{lm}\rangle}, \quad (8)$$

where  $P_{\tau l}$  stands for the radial atomic pseudowave function for the  $\tau$ th atom, and  $V_{\tau l}^{\text{ps}}$  stands for the radial pseudopotential.  $Y_{lm}$  is the spherical harmonics. Since a power product of  $V_{\tau lm}^{\text{ps}}(\mathbf{r})$  can be written as

$$\{V_{\tau lm}^{\text{ps}}(\mathbf{r})\}^n = \frac{V_{\tau l}^{\text{ps}} |P_{\tau l} Y_{lm}\rangle \langle P_{\tau l} Y_{lm} | V_{\tau l}^{\text{ps}} V_{\tau l}^{\text{ps}} |P_{\tau l} Y_{lm}\rangle^{n-1} \langle P_{\tau l} Y_{lm} | V_{\tau l}^{\text{ps}}}{\langle P_{\tau l} Y_{lm} | V_{\tau l}^{\text{ps}} | P_{\tau l} Y_{lm}\rangle^n} \quad (9)$$

for  $n \geq 1$ , the exponential of  $V_{\tau lm}^{\text{ps}}(\mathbf{r})$  can be analytically given as

$$\exp[x V_{\tau lm}^{\text{ps}}(\mathbf{r})] = 1 + \frac{V_{\tau l}^{\text{ps}} |P_{\tau l} Y_{lm}\rangle \left\{ \exp \left[ x \frac{\langle P_{\tau l} Y_{lm} | V_{\tau l}^{\text{ps}} V_{\tau l}^{\text{ps}} |P_{\tau l} Y_{lm}\rangle}{\langle P_{\tau l} Y_{lm} | V_{\tau l}^{\text{ps}} | P_{\tau l} Y_{lm}\rangle} \right] - 1 \right\} \langle P_{\tau l} Y_{lm} | V_{\tau l}^{\text{ps}}}{\langle P_{\tau l} Y_{lm} | V_{\tau l}^{\text{ps}} | P_{\tau l} Y_{lm}\rangle}. \quad (10)$$

In applying this scheme, it is necessary to express the projectors, e.g.,  $V_{\tau lm}^{\text{ps}} |P_{\tau l} Y_{lm}\rangle$ , and to compute the matrix elements, e.g.,  $\langle P_{\tau l} Y_{lm} | V_{\tau l}^{\text{ps}} | P_{\tau l} Y_{lm}\rangle$ , within the same representation, whether reciprocal space or real space, so that both sides of Eq. (9) are numerically exactly equated. Otherwise, the unitarity and conservation of the total energy are badly affected. Note that the  $V_{\tau l}^{\text{ps}}$  are not commutable to each other when the pseudopotentials belonging to different atoms overlap. The condition of nonoverlapping was previously considered necessary to apply the split-operator method,<sup>27</sup> but that is not the case here.

To summarize, the wave function at  $t + \Delta t$  to the  $n$ th order of  $\Delta t$  is

$$\psi(t + \Delta t) = U(t + \Delta t, t) \psi(t) = \left[ \prod_i S_2(p_i \Delta t; t_i) \right] \psi(t),$$

$$\begin{aligned} S_2(p \Delta t; t) &= \exp \left[ -\frac{1}{2} i T p \Delta t \right] \\ &\times \left\{ \prod_{\tau lm}^{\text{ascending}} \exp \left[ -\frac{1}{2} i V_{\tau lm}^{\text{ps}}(t) p \Delta t \right] \right\} \\ &\times \exp[-i V_{\text{Hxc}}(t) p \Delta t] \\ &\times \left\{ \prod_{\tau lm}^{\text{descending}} \exp \left[ -\frac{1}{2} i V_{\tau lm}^{\text{ps}}(t) p \Delta t \right] \right\} \\ &\times \exp \left[ -\frac{1}{2} i T p \Delta t \right], \end{aligned} \quad (11)$$

where the multiplication is done symmetrically by first arranging the pseudopotentials in ascending order of  $\tau lm$  and then in descending order.

Using the wave function, the charge density at  $t + \Delta t$  is given as

$$\rho(\mathbf{r}, t + \Delta t) = \sum_i |\psi_i(\mathbf{r}, t + \Delta t)|^2. \quad (12)$$

Generally, the Hartree-exchange-correlation potential  $V_{\text{Hxc}}(t + \Delta t)$  constructed from the charge density is not consistent with the one used for the time evolution of  $\psi$  [Eq. (11)], in that they discontinuously match at  $t + \Delta t$ . Thus, we reconstructed the potentials between  $t$  and  $t + \Delta t$  so that they would be continuously matched at  $t + \Delta t$ , and this procedure was repeated until the matching was realized self-consistently. For the electron-ion dynamics, the Hellmann-Feynman force obtained by the self-consistently determined wave function  $\psi$  is used for the Newton equation of ions at each time step.

### C. Railway curve interpolation scheme

In the reconstruction of the potential, the selection of the interpolation scheme is an important decision. The usual predictor corrector (PC) scheme uses  $n + 1$  past potentials ( $n$  is usually 1–3), and interpolation is done using an  $n$ th-order polynomial as

$$V(s) = \sum_{i=-n+1}^1 c_i(s) V(t + i\Delta t), \quad (13)$$

where the parameters  $c_i$  are determined so as to reproduce the potentials at each time slice. This procedure breaks the time-reversal symmetry, except for the second-order scheme, because a larger weight is put on the past. However, the time-reversal symmetry is known to be very important for numerical stability,<sup>21,22</sup> and to keep the symmetry, we propose using the railway curve interpolation scheme,<sup>19</sup>

$$\begin{aligned} V(s) = & \left( \frac{s-t-\Delta t}{\Delta t} \right)^2 \\ & \times \left[ 3V(t) + \Delta t \dot{V}(t) + \frac{s-t-\Delta t}{\Delta t} [2V(t) + \Delta t \dot{V}(t)] \right] \\ & + \left( \frac{s-t}{\Delta t} \right)^2 \left[ 3V(t+\Delta t) - \Delta t \dot{V}(t+\Delta t) \right. \\ & \left. - \frac{s-t}{\Delta t} [2V(t+\Delta t) + \Delta t \dot{V}(t+\Delta t)] \right] \end{aligned} \quad (14)$$

for  $s$  between  $t$  and  $t + \Delta t$ , where  $\dot{V}$  is the time derivative of the potential. This reproduces the potential up to the first time derivative at  $t$  and  $t + \Delta t$ , and is accurate to the third order of  $\Delta t$ . The time derivative of the potential can be analytically obtained if we use the TD Kohn-Sham equation as follows. Using the derivative of the charge density,

$$\begin{aligned} \dot{\rho}(\mathbf{r}, t) = & -i \sum_n \varphi_n^*(\mathbf{r}, t) H \varphi_n(\mathbf{r}, t) + i \sum_n \varphi_n(\mathbf{r}, t) H \varphi_n^*(\mathbf{r}, t) \\ = & -i \sum_n \varphi_n^*(\mathbf{r}, t) T \varphi_n(\mathbf{r}, t) + i \sum_n \varphi_n(\mathbf{r}, t) T \varphi_n^*(\mathbf{r}, t) \\ = & 2 \operatorname{Im} \left[ \sum_n \varphi_n^*(\mathbf{r}, t) T \varphi_n(\mathbf{r}, t) \right], \end{aligned} \quad (15)$$

the derivative of the potential can be obtained as

$$\dot{V}_{\text{Hxc}}(\mathbf{r}, t) = \frac{\delta V_{\text{Hxc}}[\rho(\mathbf{r}, t)]}{\delta \rho(\mathbf{r}, t)} \dot{\rho}(\mathbf{r}, t). \quad (16)$$

Averaging the interpolated potential between  $t_{j-1}$  and  $t_j$ , we obtain the value used for  $V(t_j)$  in Eq. (11).<sup>28</sup> As we will show in the next section, the RW scheme prevents the total energy from drifting, allowing us to use a much larger time step than that allowed when using the PC scheme.

### D. Cutoff

To further increase the time step  $\Delta t$ , we can smooth the charge density and the kinetic energy by cutting off highly oscillating components in real space to reduce the amplitude of high-frequency components in real time. This is based on the close relationship between the real space and real time for the high-frequency components of the wave function, which has the form

$$\exp[i\mathbf{G}\mathbf{r} - i\omega(\mathbf{G})t]. \quad (17)$$

In this equation,  $\omega$  is approximately equal to the Fourier component of the diagonal part of the Hamiltonian, and is  $\mathbf{G}^2/2$  for particularly large values of  $\mathbf{G}$ . Therefore the amplitude of high-frequency components in real time can be reduced by cutting off the large  $\mathbf{G}$  component.

High-frequency Fourier terms of the kinetic energy operator are cut off by modifying as

$$T(\mathbf{G}) = \min \left[ \frac{\mathbf{G}^2}{2}, E_{\text{prec}} \right]. \quad (18)$$

This is essentially the same as the preconditioning technique developed for the Car-Parrinello type MD.<sup>17</sup> Similarly, the high-frequency component of the potential can be reduced in magnitude by smoothing the charge density in reciprocal space,

$$\bar{\rho}(\mathbf{G}) = \rho(\mathbf{G}) f_{\text{cut}}(\mathbf{G}), \quad (19)$$

$$f_{\text{cut}}(\mathbf{G}) = \frac{1}{1 + \exp[\beta(\mathbf{G}^2/2 - E_{\text{cut}})]}. \quad (20)$$

The potential, which is a function of  $\rho$ , then becomes smooth. This mimics the standard plane-wave scheme where the cutoff is introduced by the step function as

$$\bar{\rho}(\mathbf{G}) = \rho(\mathbf{G}) \Theta \left( E_{\text{cut}} - \frac{\mathbf{G}^2}{2} \right). \quad (21)$$

We use a smooth function because, contrary to the plane-wave scheme formulated in reciprocal space only, our

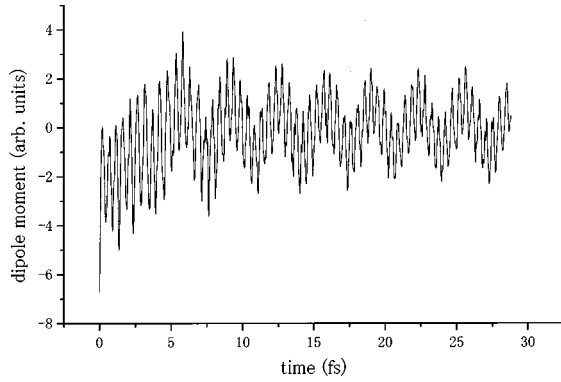


FIG. 1. Typical time evolution of the dipole moment, which is a superposition of the intra-atomic depolarization having a period of 2.3 fs and the interatomic charge transfer having a period of 21 fs. Parameters used in this calculation were  $\Delta t=1.0$  a.u., the RW scheme, fourth-order Suzuki-Trotter decomposition,  $E_{\text{prec}}=6$  Ry, and  $E_{\text{cut}}=20$  Ry.

scheme is formulated both in reciprocal space (for  $T$ ) and real space (for  $V$ ). Such a dual-space treatment is required by the split-operator scheme where  $T$  and  $V$  are diagonal in reciprocal space and real space, respectively. In that case,  $\bar{\rho}(\mathbf{r})$  obtained by Fourier transforming  $\bar{\rho}(\mathbf{G})$  can become negative unless a smooth cutoff is introduced. We have found that a suitable value for the smoothing factor  $\beta$  is between 0.5 and 1.0 a.u.

### III. RESULTS

In this section we evaluate the performance of the above techniques by applying them to a simple model of the electron dynamics of  $\text{Al}_2$  and a model of the electron-ion dynamics of  $\text{K}_3$ .

#### A. Electron dynamics of $\text{Al}_2$

In our first example, we located two aluminum atoms 6 bohrs apart and keeping the interatomic distance constant we followed the electronic motion for up to 720 fs, which corresponds to 30 000 time steps when  $\Delta t=1$  a.u. We started the simulation slightly shifted from the ground state by initially applying a uniform electric field parallel to the molecular axis. The electric field, whose strength was 0.5 eV/bohr, was then suddenly switched off when starting the simulation. The electronic motion had two main degrees of freedom: the interatomic charge transfer and the intraatomic depolarization associated with rehybridization of the  $3s$  and  $3p_z$  orbitals. Because of the large interatomic distance (6 bohrs), the two motions had different time constants, 21 fs and 2.3 fs, for the interatomic and intra-atomic motion, respectively. Because of this, the total dipole moment behaved as shown in Fig. 1. Such two-mode motion is generally considered to appear, for example, in the transfer of electrons in the collision of heavy molecules or in tunneling in nanostructures. We will now explain in detail how the above techniques improve the numerical stability and efficiency. In the following electron dynamics of  $\text{Al}_2$ , the local pseudopotential of Pickett, Louie, and Cohen<sup>29</sup> was used to reduce the CPU time. The smoothing factor for the cutoff function  $\beta$  was taken to be 1.0 a.u.

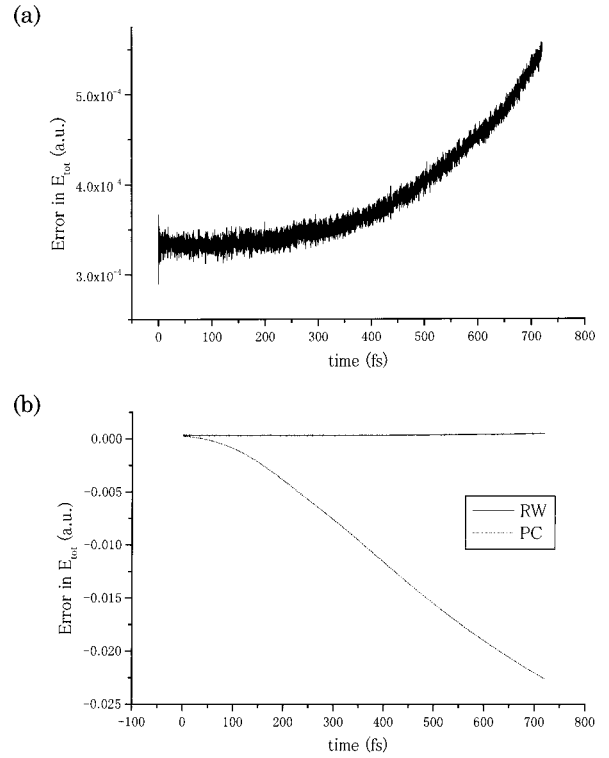


FIG. 2. Typical time evolution of the error in the total energy, which consists of very fast fluctuation and long time-scale drift. The drift shows a superlinear dependence on time (a). When the RW scheme was used [see (a) and the solid line in (b)], the drift became significantly smaller than that when the PC scheme was used [see the broken line in (b)]. Parameters used in this calculation were  $\Delta t=1.0$  a.u., fourth-order Suzuki-Trotter decomposition,  $E_{\text{prec}}=6$  Ry, and  $E_{\text{cut}}=20$  Ry. Note that the energy scale of (a) is much smaller than that of (b).

#### 1. Railway curve versus the conventional predictor corrector

In this subsection we compare the results obtained using the railway curve interpolation scheme and those obtained using the conventional predictor corrector interpolation scheme. We have found that the difference mainly appears in the conservation of the total energy. Figure 2 shows how the error in the total energy,  $E_{\text{tot}}(t) - E_{\text{tot}}(t=0)$ , evolved with time. Parameters used in this calculation were  $\Delta t=1.0$  a.u., the RW scheme, fourth-order Suzuki-Trotter formula,  $E_{\text{prec}}=6$  Ry, and  $E_{\text{cut}}=20$  Ry. The error consisted of long time-scale drift and very short time-scale fluctuation. The drift often increased exponentially as shown in Fig. 2(a), indicating that the quality of the simulation can quickly deteriorate over the simulation. After 600 fs, we found that the drift was about  $5 \times 10^{-4}$  a.u. ( $=0.01$  eV) when the RW scheme was used, while it was 0.02 a.u. ( $=0.54$  eV) when the PC scheme was used [see Figs. 2(a) and 2(b)]. Since this amount, 0.54 eV, is almost the same as the typical energy scale of these dynamics, the present simulation using the PC scheme is meaningless except for the initial part.

Next we systematically investigated the drift by changing the time step  $\Delta t$  between 0.03 and 1.0 a.u. (Fig. 3). The conservation of the total energy was roughly 100 times better for the RW scheme. Since the computational time required when using each scheme is almost the same, the relative merit of the RW scheme is obvious.

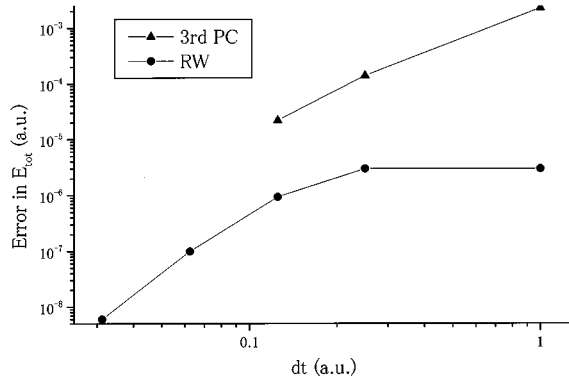


FIG. 3. The error in the total energy at  $t=143$  fs plotted against  $\Delta t$ . The error for the RW scheme is approximately 100 times smaller than that for the PC scheme. Parameters used in this calculation were the fourth-order Suzuki-Trotter decomposition,  $E_{\text{prec}}=6$  Ry and  $E_{\text{cut}}=20$  Ry.

When we used the fourth-order PC scheme instead of the third-order PC scheme used to obtain Fig. 2(b), though, the conservation became worse. Since the asymmetry is larger for the fourth-order scheme, we believe the time-reversal symmetry plays an important role in the drift of the total energy.

Some additional remarks concerning the error of the total energy: The fluctuation of the total energy was almost completely independent of the interpolation scheme, but had large dependence on the order of the Suzuki-Trotter decomposition as is shown in Fig. 4. On the contrary, the drift was almost insensitive to the order of the decomposition but was sensitive to the scheme of the interpolation. This means that what was reduced by improving the Schrödinger equation solver was not the drift, which tends to induce numerical instability, but the fluctuation, which does not induce instability.

## 2. Lower order versus higher order

We also investigated Suzuki-Trotter decompositions of different orders, i.e., second-, fourth-, sixth-, and eighth-order schemes. We found that the difference mainly appeared in the time evolution of the dipole moment. In Fig. 5, we plotted the time evolution of the dipole moment referred to a result obtained using small  $\Delta t$  which was equal to

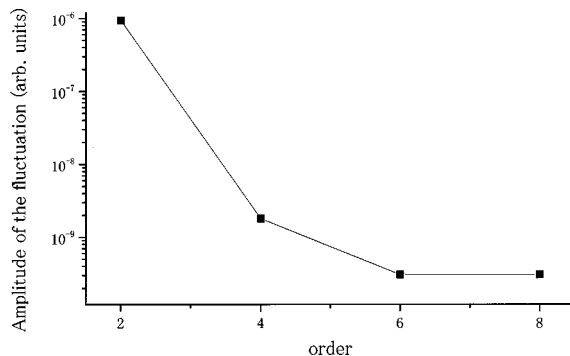


FIG. 4. Fluctuation of the total energy curve at  $t=72$  fs plotted against the order of the Suzuki-Trotter decomposition. Parameters used in this calculation were  $\Delta t=1$  a.u., the RW scheme,  $E_{\text{prec}}=6$  Ry, and  $E_{\text{cut}}=20$  Ry.

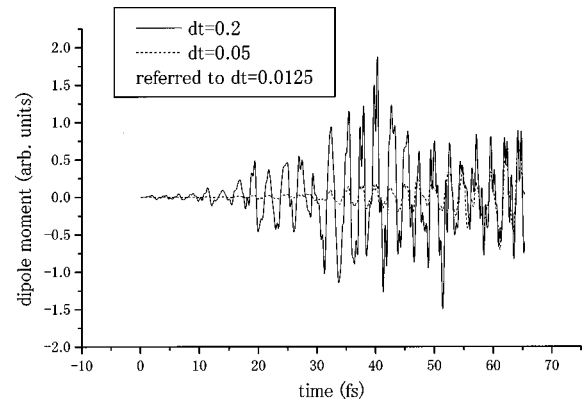


FIG. 5. Typical time evolution of error in the dipole moment. Parameters used in this calculation were the RW scheme, second-order Suzuki-Trotter decomposition,  $E_{\text{prec}}=6$  Ry, and  $E_{\text{cut}}=20$  Ry.

0.0125 a.u. Parameters used in this calculation were the RW scheme, second-order Suzuki-Trotter formula,  $E_{\text{prec}}=6$  Ry, and  $E_{\text{cut}}=20$  Ry. The deviation increased exponentially until it became as large as the absolute dipole moment which was roughly equal to 2 in our arbitrary units (see Fig. 1). This happened at about 20 fs for  $\Delta t=0.2$  a.u. and at about 60 fs for  $\Delta t=0.05$  a.u. The phase information regarding intra-atomic motion was then obviously lost.

In Fig. 6, we plotted the accumulation of the error for  $\Delta t$  of 0.05 or 0.2 a.u. and the second- and the fourth-order Suzuki-Trotter decomposition. Compared with the simulation using the second-order Suzuki-Trotter decomposition and  $\Delta t=0.05$  a.u., the simulation using the fourth-order Suzuki-Trotter decomposition and  $\Delta t=0.2$  a.u. improved the accuracy by two orders of magnitude without significantly increasing the computational time. Since the computational time when going from the second- to the fourth-order scheme with the same  $\Delta t$  of 0.05 a.u. is only a factor of 5, it is advantageous to use a fourth-order scheme.

One might consider that using a still higher-order scheme, such as sixth and eighth order, would yield a more accurate simulation, but this was not true in our case. No improvement in the accuracy was found. This was probably due to the self-consistent field (SCF) potential whose accuracy is

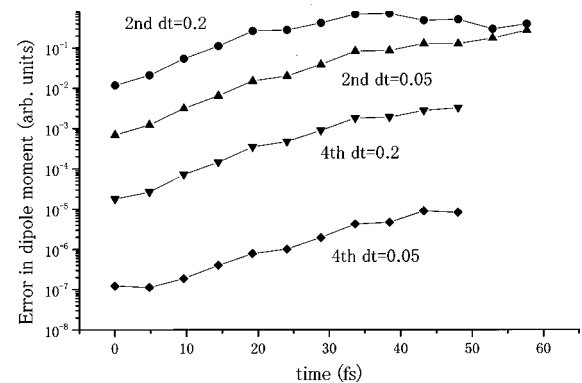


FIG. 6. The error in the dipole moment at  $t=142$  fs obtained for different  $\Delta t$ 's or orders of the Suzuki-Trotter decomposition. Parameters used in this calculation were the RW scheme,  $E_{\text{prec}}=6$  Ry, and  $E_{\text{cut}}=20$  Ry.

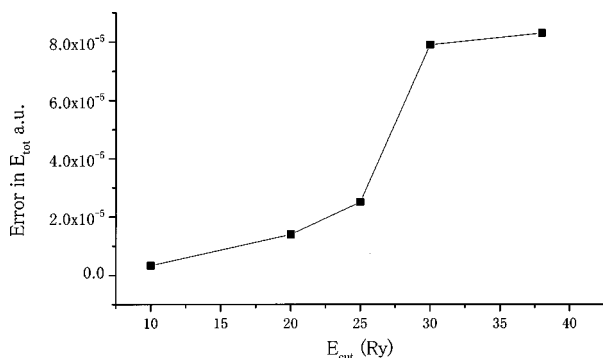


FIG. 7. The error in the total energy at  $t=142$  fs plotted against the  $E_{\text{cut}}$ . Parameters used in this calculation were  $\Delta t=0.2$  a.u., the RW scheme, and  $E_{\text{prec}}=6$  Ry.

limited also by the order of the interpolation scheme. However, when a non-SCF potential is used, a sixth-order scheme was superior to the fourth-order scheme.

We have found, however, that the accuracy of the interpolation cannot be improved by simply increasing the order of the polynomial [see Eq. (14)]. When a fifth-order polynomial was used to reproduce the potential up to the second derivative, the accuracy of the dipole moment and the conservation of the total energy became worse. We also found that when a second-order interpolation scheme was used, the accuracy and the conservation again became worse. Therefore the third-order scheme is the most suitable when using the RW scheme.

### 3. Cutoff

When we compared simulations with and without the preconditioning and the cutoff techniques, we found that a difference appeared in the conservation of the total energy. First, we changed only the cutoff energy of the charge density with the preconditioning energy fixed at 6 Ry. When we compared the error in the total energy at  $t=142$  fs, the error increased as the cutoff energy was increased (Fig. 7). Parameters used in this calculation were  $\Delta t=0.2$  a.u., the third RW, and the fourth Suzuki-Trotter decomposition. Next, we compared the error in the total energy by changing the  $E_{\text{cut}}$ ,  $E_{\text{prec}}$ , and  $\Delta t$  (Fig. 8). When  $\Delta t$  was smaller than 0.3 a.u., the error had very little dependence on  $E_{\text{cut}}$  and  $E_{\text{prec}}$ ,

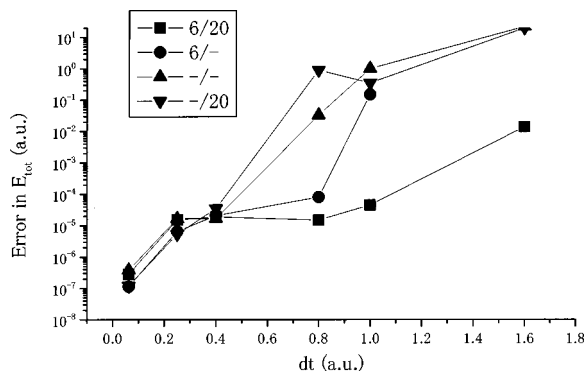


FIG. 8. The error in the total energy at  $t=142$  fs versus the  $E_{\text{prec}}$  and  $E_{\text{cut}}$ . “6/20,” for example, indicates  $E_{\text{prec}}=6$  Ry and  $E_{\text{cut}}=20$  Ry, and “-/-” means neither the preconditioning nor the cutoff were used. The RW scheme was used in this calculation.

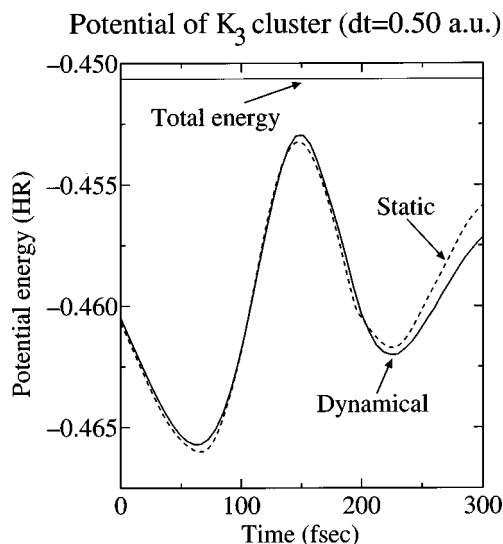


FIG. 9. Calculated potential energy surface (PES) during the molecular dynamics simulation for  $K_3$ . The solid line is the PES obtained by dynamical calculation while the dotted line is the Born-Oppenheimer surface obtained at the corresponding atomic configurations. The total energy curve is also plotted in the figure.

but when  $\Delta t$  was larger, the dependence became strong. The simulation without the preconditioning showed poor conservation of the total energy for  $0.4 < \Delta t \leq 0.8$  a.u. For  $\Delta t = 1$  a.u., only the simulation with both the preconditioning and the cutoff of the charge density was stable.

### B. Electron-ion dynamics of $K_3$

Next, we studied the numerical stability and efficiency of the mixed electron-ion dynamics by following the coupled TD-DFT and Newton equation. We simulated the dynamics of a photoexcited  $K_3$  cluster. Initially, we excited the electron from the ground state  $(a_1)^2(b_1)^1$  to an excited state  $(a_1)^2(5a_1)^1$  and let the K atoms have velocities equal to one-tenth of the Hellmann-Feynman force in atomic units. To break the initial symmetry ( $C_{2v}$ ), we randomly displaced the atomic position by 0.1 a.u. The simulation was done for 300 fs. In this calculation, we adopted the nonlocal pseudopotential of Troullier and Martins,<sup>30</sup> and the potential-partitioning technique was used to avoid the ghost effect.<sup>31</sup> We used the third-order RW scheme, the fourth-order Suzuki-Trotter decomposition,  $E_{\text{prec}}=8$  Ry, and  $E_{\text{cut}}=8$  Ry. The parameter for the cutoff function  $\beta$  was taken to be 0.5 a.u. In each time step, the atomic positions were also updated using the Verlet algorithm.

The drift in the total energy at 300 fs was  $1.0 \times 10^{-8}$  a.u. when we used  $\Delta t=0.1$  a.u. and it was  $1.0 \times 10^{-7}$  when we used  $\Delta t=0.5$  a.u. On the other hand, when the PC scheme was used instead of the RW scheme, the total energy increased very quickly at about 250 fs and the simulation encountered serious numerical instability. This was not improved when  $\Delta t$  was reduced to 0.05 a.u. In this way, the advantage of the RW scheme became very apparent in this simulation.

We found that at about 250 fs, the deviation from the Born-Oppenheimer surface (BOS) became appreciable, as shown in Fig. 9, which is plotted on the basis of the simula-

tion using  $\Delta t=0.5$  a.u. In this figure, we plotted the total potential energy, which is equal to the sum of the kinetic energy, the Hartree-exchange-correlation energy, the pseudopotential energy, and the ion-ion interactions, against time. Deviation from the BOS can be seen in the difference in the total potential energy between the state evolving with time (the solution of the TD-DFT) and the state of which the electronic degrees of freedom were optimized at each time step. Deviation from the BOS directly indicates the mixture of two or more electronic eigenstates, which results in a fluctuation of the charge density. This makes numerical condition more demanding. We believe this triggered the instability of the simulation using the PC scheme.

In this calculation, the initial state was  $(a_1)^2(5a_1)^1$ , which had an excitation energy of 1.61 eV. This state was chosen because we expected it to have a large oscillator strength on the basis of a symmetry consideration and because the excitation energy is close to the experimental one, 1.54 eV.<sup>32</sup> Experimentally, the excited cluster dissociated into  $K+K_2$  about 500 fs after the excitation. In our simulation we found a deviation from the BOS at 250 fs, by which time the cluster geometry had changed from a triangle with angles of  $81^\circ$ ,  $49.5^\circ$ , and  $49.5^\circ$  (the initial geometry) to a triangle with angles of  $52.0^\circ$ ,  $57.5^\circ$ , and  $69.6^\circ$ . We stopped

the simulation at that point since the branching becomes significant there. Thus we do not know if the simulation would lead to a dissociation or not. It would be interesting to continue the simulation by adopting the surface hopping prescription, but that is beyond the scope of this paper.

#### IV. CONCLUSION

We have proposed schemes that enable stable and efficient simulation of electron or electron-ion dynamics within the TD-DFT and pseudopotentials. We have found that by using a combination of techniques, RW interpolation for updating the self-consistent potential and smoothing of the kinetic and potential energy operators, the numerical instability problem can be eliminated and a larger time step can be used for the integration. This opens the possibility of performing subpicosecond-long simulations on transient dynamics of electrons and ions for a number of materials.

#### ACKNOWLEDGMENTS

We are indebted to Roberto Car for his suggestions concerning the branching problem. All calculations were done using the SX-4 supercomputer system at the NEC Tsukuba Research Laboratories.

<sup>1</sup>See, for example, R. N. Zare, *Science* **279**, 1875 (1998).

<sup>2</sup>See, for example, J. Shah, *Ultrafast Spectroscopy of Semiconductors and Semiconductor Nanostructures* (Springer, Berlin, 1996).

<sup>3</sup>E. Runge and E. K. U. Gross, *Phys. Rev. Lett.* **52**, 997 (1984).

<sup>4</sup>A. Nakano, R. K. Kalia, and P. Vashishta, *Phys. Rev. B* **44**, 8121 (1991).

<sup>5</sup>U. Saalman and R. Schmidt, *Phys. Rev. Lett.* **80**, 3213 (1998).

<sup>6</sup>K. Yabana and G. F. Bertsch, *Phys. Rev. B* **54**, 4484 (1996).

<sup>7</sup>G. Vignale and W. Kohn, *Phys. Rev. Lett.* **77**, 2037 (1996).

<sup>8</sup>G. Vignale, C. A. Ullrich, and S. Conti, *Phys. Rev. Lett.* **79**, 4878 (1997).

<sup>9</sup>E. K. U. Gross, C. A. Ullrich, and U. J. Grossmann, in *Density Functional Theory*, edited by E. K. U. Gross and R. M. Dreizler (Plenum Press, New York, 1995), p. 149.

<sup>10</sup>J. B. Delos and W. R. Thorson, *Phys. Rev. A* **6**, 720 (1972).

<sup>11</sup>O. V. Prezhdo and P. J. Rossky, *J. Chem. Phys.* **107**, 825 (1997).

<sup>12</sup>J. C. Tully and R. K. Preston, *J. Chem. Phys.* **55**, 217 (1971).

<sup>13</sup>O. V. Prezhdo and P. J. Rossky, *J. Chem. Phys.* **107**, 825 (1997).

<sup>14</sup>U. Muller and G. Stock, *J. Chem. Phys.* **107**, 6230 (1997).

<sup>15</sup>See also the pioneering work by A. Selloni, P. Carnevali, R. Car, and M. Parrinello, *Phys. Rev. Lett.* **59**, 823 (1987).

<sup>16</sup>R. Car and M. Parrinello, *Phys. Rev. Lett.* **55**, 2471 (1985).

<sup>17</sup>F. Tassone, F. Mauri, and R. Car, *Phys. Rev. B* **50**, 10 561 (1994).

<sup>18</sup>M. Suzuki, *J. Phys. Soc. Jpn.* **61**, L3015 (1992); M. Suzuki and T. Yamauchi, *J. Math. Phys.* **34**, 4892 (1993).

<sup>19</sup>M. Iri and Y. Fujino, *Common Sense for Numerical Calculation* (Kyoritsu, Tokyo, 1985), p. 116 (in Japanese). See also, H. Akima, *J. Assoc. Comput. Mach.* **17**, 589 (1970).

<sup>20</sup>M. D. Feit, J. A. Fleck, and A. Steiger, *J. Comput. Phys.* **47**, 412 (1982); M. D. Feit and J. A. Fleck, *J. Chem. Phys.* **78**, 301 (1982).

<sup>21</sup>R. Kosloff, *J. Phys. Chem.* **92**, 2087 (1988).

<sup>22</sup>T. Iitaka, *Phys. Rev. E* **49**, 4684 (1994).

<sup>23</sup>H. Yoshida, *Phys. Lett. A* **150**, 262 (1990).

<sup>24</sup>M. Suzuki, *Proc. Jpn. Acad., Ser. B: Phys. Biol. Sci.* **69**, 161 (1993), and references therein.

<sup>25</sup>K. Takahashi and K. Ikeda, *J. Chem. Phys.* **99**, 8680 (1993).

<sup>26</sup>L. Kleinmann and D. M. Bylander, *Phys. Rev. Lett.* **48**, 1425 (1982).

<sup>27</sup>J. Theilhaber, *Phys. Rev. B* **46**, 12 990 (1992).

<sup>28</sup>Alternatively, this can be computed by taking a numerical differentiation.

<sup>29</sup>W. E. Pickett, S. G. Louie, and M. L. Cohen, *Phys. Rev. B* **17**, 815 (1977).

<sup>30</sup>N. Troullier and J. L. Martins, *Solid State Commun.* **74**, 613 (1990); *Phys. Rev. B* **43**, 1993 (1990).

<sup>31</sup>M. Saito, O. Sugino, and A. Oshiyama, *Phys. Rev. B* **46**, 2606 (1992).

<sup>32</sup>S. Rutz, H. Ruppe, E. Schreiber, and L. Wöste, *Z. Phys. D* **40**, 25 (1996); H. Ruppe, S. Rutz, E. Schreiber, and L. Wöste, *Chem. Phys. Lett.* **257**, 356 (1996).